Atmospheric
Chemistry
and Physics

Supplement of

Regional influence of wildfires on aerosol chemistry in the western US and insights into atmospheric aging of biomass burning organic aerosol

Shan Zhou et al.

Correspondence to: Qi Zhang (dkwzhang@ucdavis.edu)

Section 1. PMF analysis

PMF is commonly applied to the organic mass spectral matrix to determine distinct OA factors (Zhang et al., 2011 and references therein), but conducting PMF analysis on the combined spectra of organic and inorganic aerosols allows for the deriving of additional information. In this study, we performed PMF analysis under various conditions, i.e., on organic matrix only and combined aerosol matrix for the entire sampling period, BB impacted periods, and clean periods without BB influence, respectively. PMF analysis on the organic matrix for "No BB" periods resolved two types of oxygenated OA (OOA) – an intermediately oxidized OOA associated with boundary layer (BL) dynamics and a highly oxidized one that correlated with sulfate and appeared to represent free tropospheric air masses. However, PMF analysis on the organic matrix for the entire study period was unsuccessful at retrieving two meaningful OOA factors. A minimum of 5 factors is needed to adequately account for the observed variance but the 5-factor solution resolved only one OOA and four other factors that appeared to represent BBOAs. However, there are indications of splitting and mixing among factors for this solution. The 6-factor solution led to further splitting and mixing of the BBOA factors without being able to resolve two meaningful OOAs. In contrast, performing PMF on the combined inorganic and organic matrix allowed the model to resolve a highly-oxidized background OOA factor associated with ammonium sulfate, an intermediately oxidized background OOA factor driven by BL dynamics, and three distinct BBOA factors for the 5-factor solution. In addition, the solutions of the combined matrix provide information on the distributions of inorganic signals among different factors and the association between inorganic and organic aerosol components in each factor. This information is helpful for interpreting the sources, chemical characteristics, and evolution processes of OA (Sun et al., 2012).

37   **Table S1.** The average ($\pm 1\sigma$) value of measured aerosol and gas phase parameters for three aerosol regimes.

	"No BB"		"BB Infl"		"BB Plm"	
	Mean	1σ	Mean	1σ	Mean	1σ
f_{60}	0.18%	0.1%	0.43%	0.05%	0.77%	0.29%
CO [c]	87.8	17.9	121.4	24.8	178.3	68.8
NR-PM$_1$ [a]	3.66	4.22	13.42	7.15	25.67	19.89
Organics [a]	3.11	3.69	12.40	6.71	24.30	18.95
Sulfate [a]	0.42	0.37	0.61	0.20	0.62	0.22
Nitrate [a]	0.03	0.03	0.15	0.12	0.35	0.47
Ammonium [a]	0.10	0.12	0.25	0.11	0.38	0.23
Chloride [a]	0.006	0.003	0.012	0.018	0.018	0.021
σ_{550nm} [b]	6.7	8.0	32.7	19.3	88.3	74.1
NO [c]	0.012	0.01	0.017	0.02	0.019	0.02
NO$_2$ [c]	0.13	0.04	0.17	0.06	0.14	0.07
PAN [c]	0.08	0.05	0.23	0.06	0.36	0.07
NO$_y$ [c]	0.44	0.07	0.75	0.08	1.03	0.22
O$_3$ [c]	44.7	0.23	49.7	0.21	47.3	0.51

38   [a] $\mu g\ m^{-3}$.
39   [b] Mm^{-1}
40   [c] ppbv

41   **Table S2.** Correlation Coefficient (r^2) between tracers and the total BBOA (= BBOA-1 + BBOA-2 + BBOA-3), as

42   well as each OA factor.

| Variables	BBOA	BBOA-1	BBOA-2	BBOA-3	BL-OOA	LV-OOA
BBOA	1					
BBOA-1	0.84	1				
BBOA-2	0.84	0.54	1			
BBOA-3	0.91	0.59	0.80	1		
BL-OOA	0.07	0.03	0.06	0.10	1	
LV-OOA	0.06	0.06	0.03	0.07	0.02	1
Organics	0.98	0.79	0.83	0.90	0.16	0.04
Sulfate	< 0.01	< 0.01	0.01	0.01	0.08	0.66
Nitrate	0.47	0.60	0.33	0.28	<0.01	0.02
Ammonium	0.63	0.51	0.57	0.56	0.07	0.12
Chloride	0.25	0.33	0.18	0.14	0.01	0.01
$C_2H_3O^+$	0.93	0.70	0.87	0.87	0.22	0.03
CO_2^+	0.87	0.57	0.79	0.95	0.21	0.02
CHO_2^+	0.93	0.67	0.91	0.90	0.15	0.01
$C_4H_9^+$	0.94	0.95	0.71	0.75	0.06	0.07
$C_2H_4O_2^+$	0.86	0.94	0.65	0.62	0.03	0.04
$C_3H_5O_2^+$	0.95	0.92	0.78	0.76	0.05	0.05
$CH_3SO_2^+$	0.34	0.22	0.31	0.38	0.47	0.02
CO	0.89	0.70	0.73	0.86	0.09	0.08
σ_{550nm}	0.93	0.77	0.74	0.90	0.08	0.09
NO	0.04	0.02	0.06	0.04	0.04	0.01
NO_2	< 0.01	< 0.01	0.01	< 0.01	0.04	0.07
NO_x	< 0.01	< 0.01	< 0.01	< 0.01	0.06	0.05
NO_y	0.75	0.67	0.59	0.66	0.09	< 0.01
PAN	0.60	0.48	0.49	0.59	0.02	0.01

43
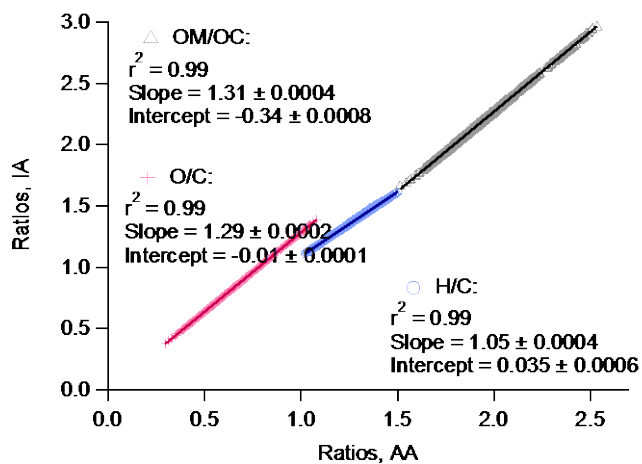
Fig. S1. Scatter plot of OM/OC, O/C, and H/C calculated with the Improved Ambient (IA) method vs. that with the Aiken-Ambient (AA) method. Data fitting was performed using the orthogonal distance regression (ODR).
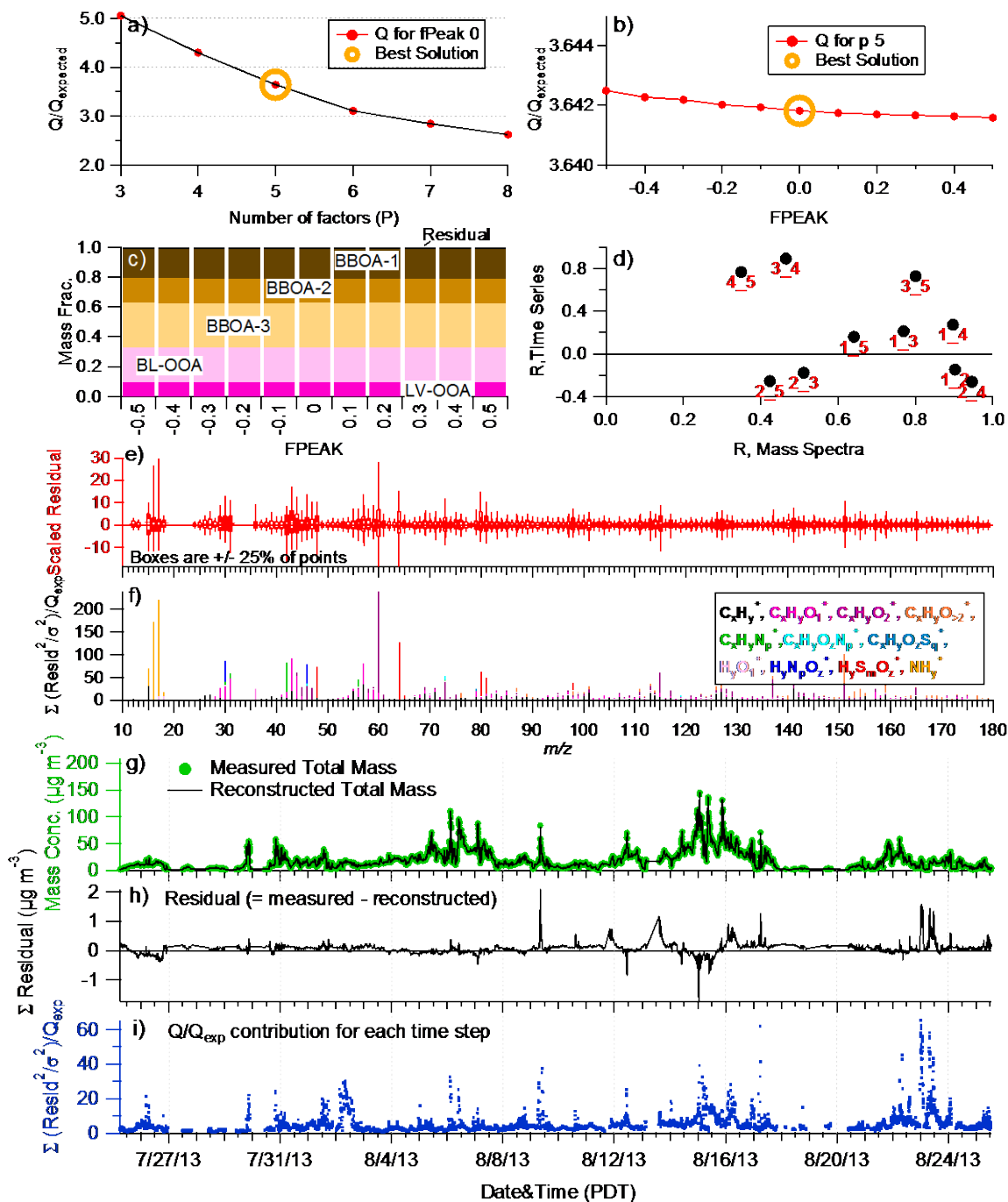
Fig. S2. Summary of the evaluation of the PMF results for the 5-factor solution: (a) Q/Q_{exp} as a function of number of factors (P), (b) Q/Q_{exp} as a function of fPeak values, (c) fractions of PMF factors as a function of fPeak values, (d) correlation between the 5 factors in terms of mass spectrum and time series (1: BL-OOA, 2: LV-OOA, 3: BBOA-2, 4: BBOA-3, 5: BBOA-1), (e) box plot of the scaled residuals for each ion, (f) Q/Q_{exp} values for each ion, (g) time series of the measured NR-PM$_1$ mass concentration and the reconstructed mass, (h) Residual time series, and (i) Q/Q_{exp} time series.

6
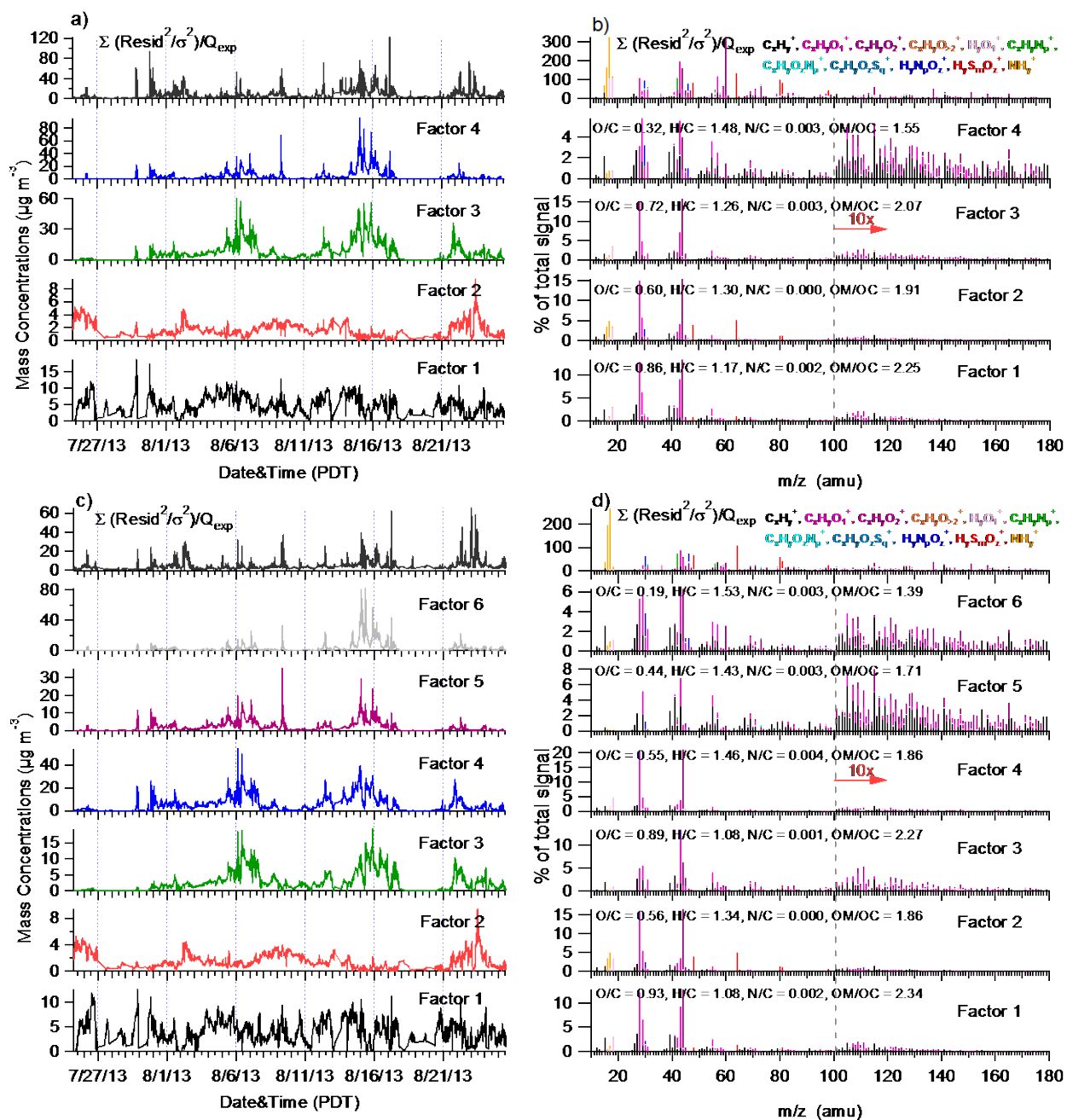
Fig. S3. The time series and mass spectral profile of total Q/Q_{exp} and each OA factor for the 4-factor (a, b) and 6-factor (c, d) solution.
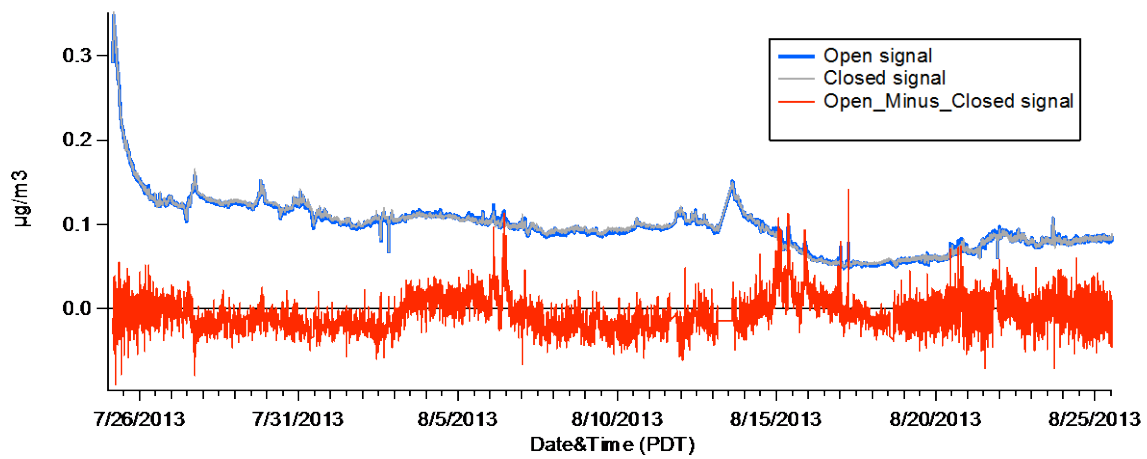
57
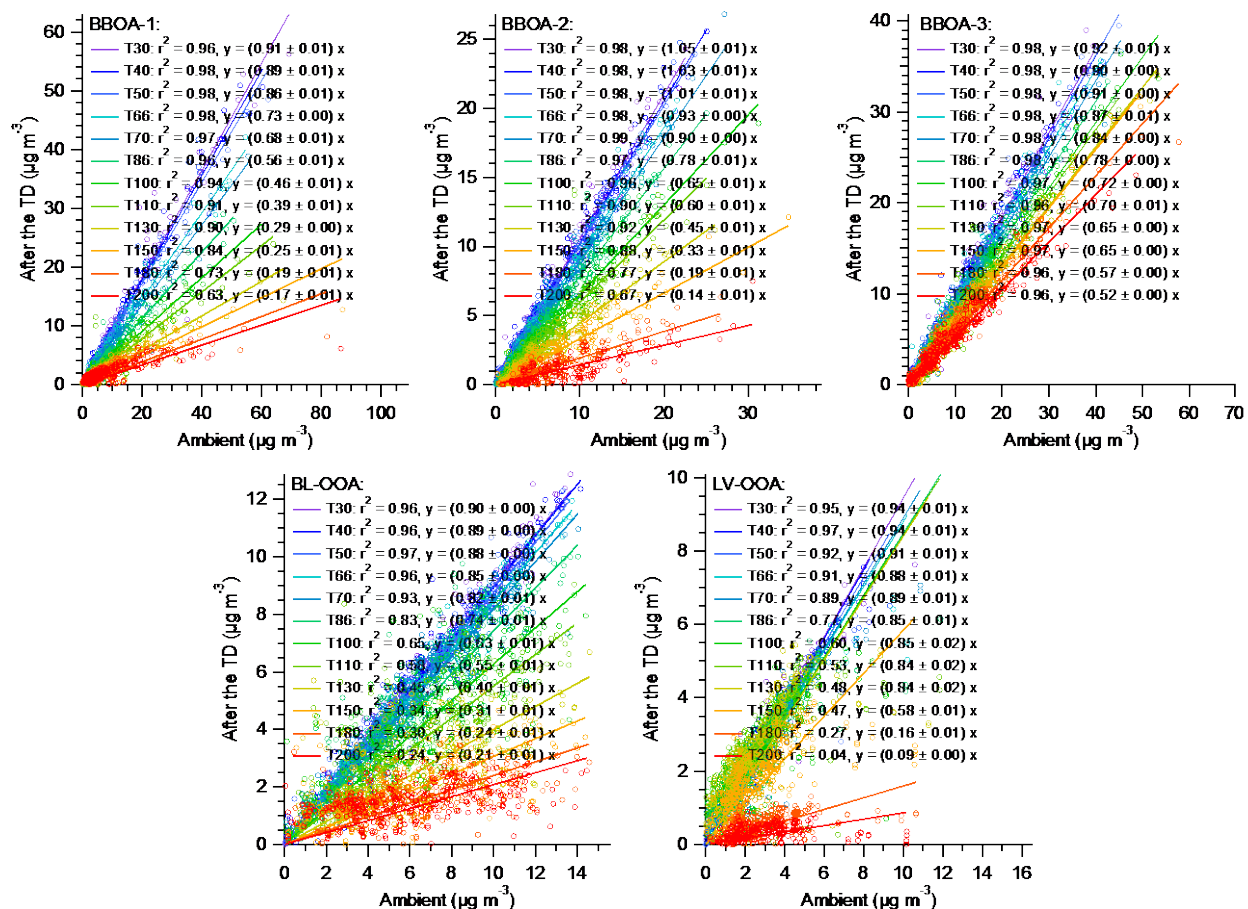
Fig. S4. Scatter plots of data after the TD vs. ambient for OA factors. Data fitting was performed using the orthogonal distance regression (ODR) forced through origin.

60
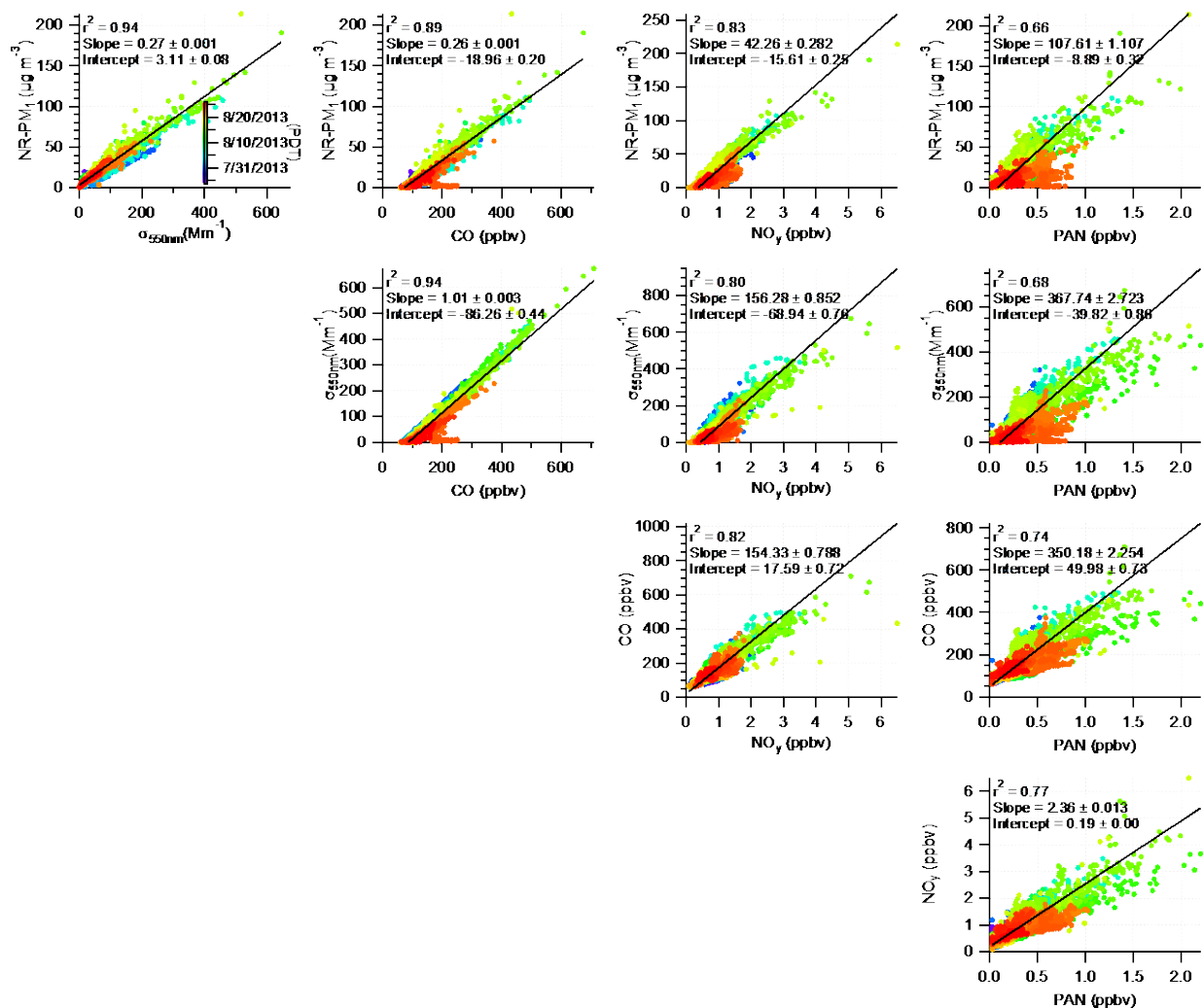
Fig. S5. Scatter plots of the cross correlations between NR-PM$_1$, σ_{550nm}, CO, NO$_y$, and PAN, colored by time.
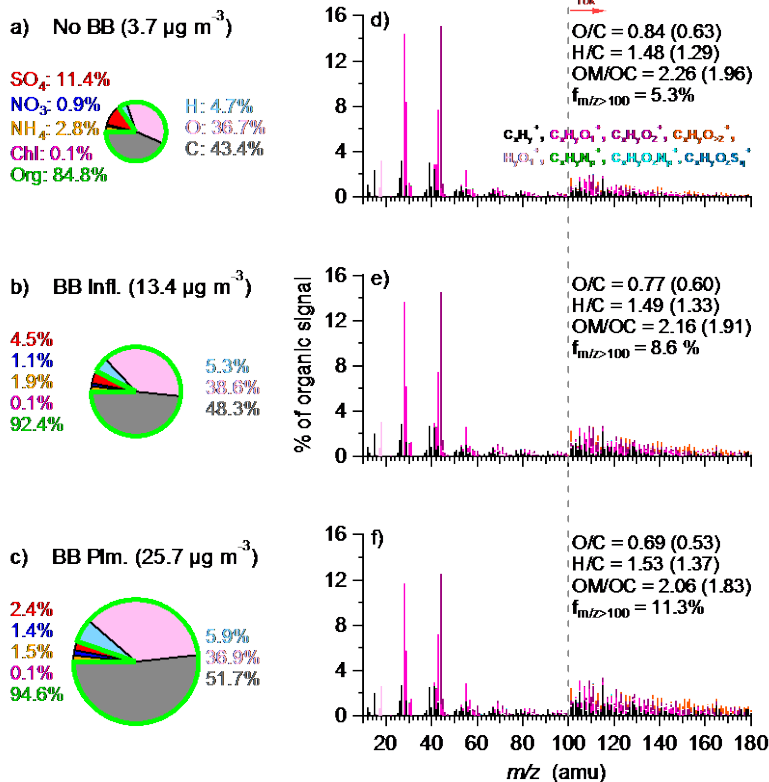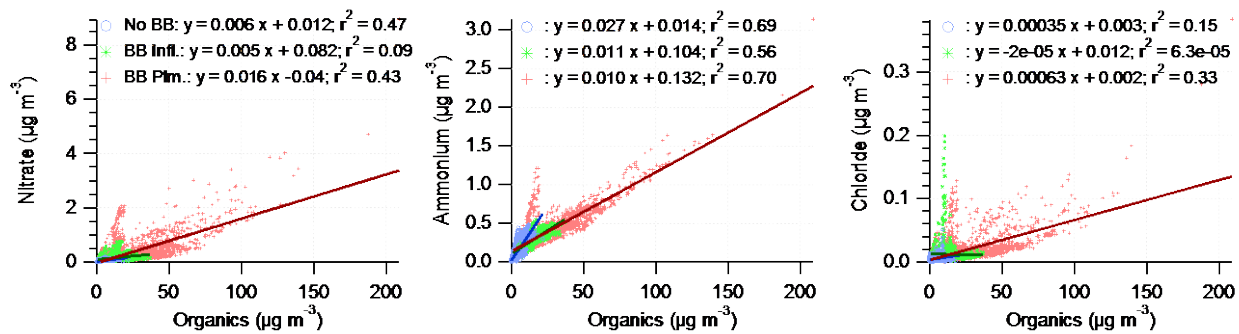Data fitting was performed using the orthogonal distance regression (ODR).

63

64 **Fig. S6.** Time series of K^+ measured by the HR-AMS in different chopper positions.

Fig. S7. The average NR-PM$_1$ composition (a-c) and OA HRMS (d-f) colored by eight ion families (i.e., C$_x$H$_y^+$, C$_x$H$_y$O$_1^+$, C$_x$H$_y$O$_2^+$, C$_x$H$_y$O$_{>2}^+$, H$_y$O$_1^+$, C$_x$H$_y$N$_p^+$, C$_x$H$_y$O$_z$N$_p^+$, and C$_x$H$_y$O$_z$S$_q^+$), for "No BB" (a and d), "BB Infl" (b and e), and "BB Plm" regimes (c and f), respectively. Organic portion in the pie charts are colored by four elements (i.e., C, O, H, and N). Numbers for in the pie charts corresponds to the mass fractional contribution of each species and element to total NR-PM$_1$ mass. The elemental ratios calculated with the IA method are shown in the legends of with those obtained using the AA method in parenthesis.
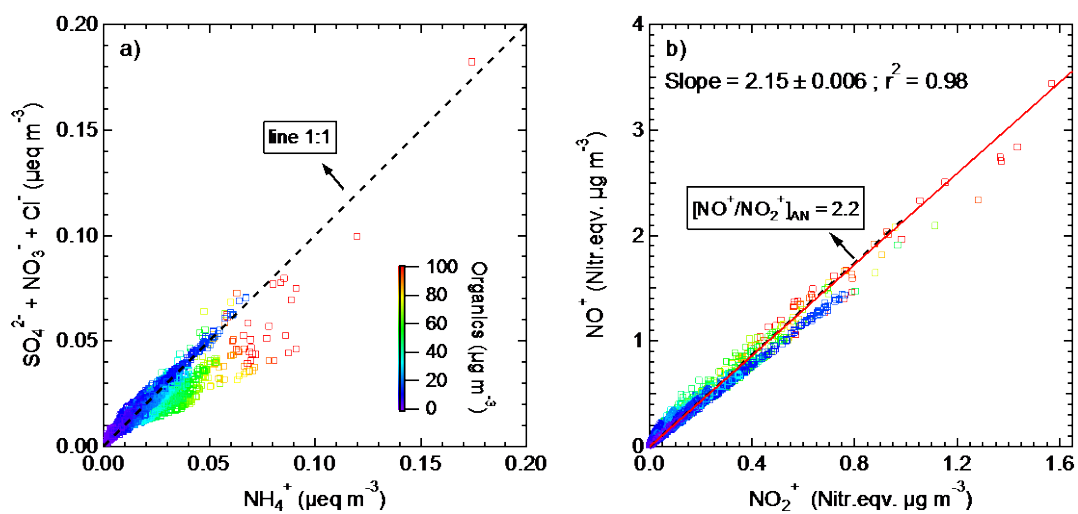
73

Fig. S8. Scatter plots of nitrate, ammonium, and chloride vs. organics for "No BB", "BB Infl", and "BB Plm" regimes, respectively. Data fitting was performed using the orthogonal distance regression (ODR).

Fig. S9. Scatter plots of (a) the sum of all anion concentration (sulfate + nitrate + chloride) vs. cation concentration (ammonium) and (b) NO^+ vs. NO_2^+ for data with $f_{60} > 0.3\%$ (i.e., "BB Infl" and "BB Plm" periods) colored by organic mass concentration. Data fitting in (b) was performed using the orthogonal distance regression (ODR) forced through origin.
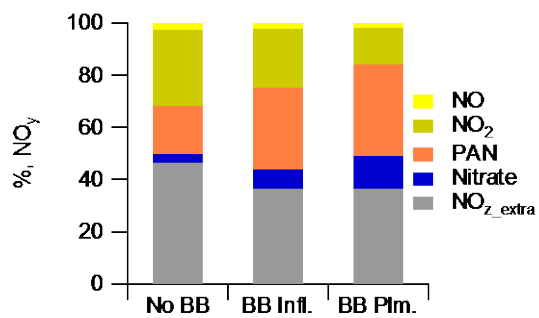
81

82 **Fig. S10.** The mass fractional contribution of nitrogen species (i.e., gas phase NO, NO_2, PAN, particle phase nitrate,
83 and the rest NO_z ($NO_{z\_extra} = NO_y - (NO + NO_2 + PAN + nitrate)$) to total NO_y for the three regimes.
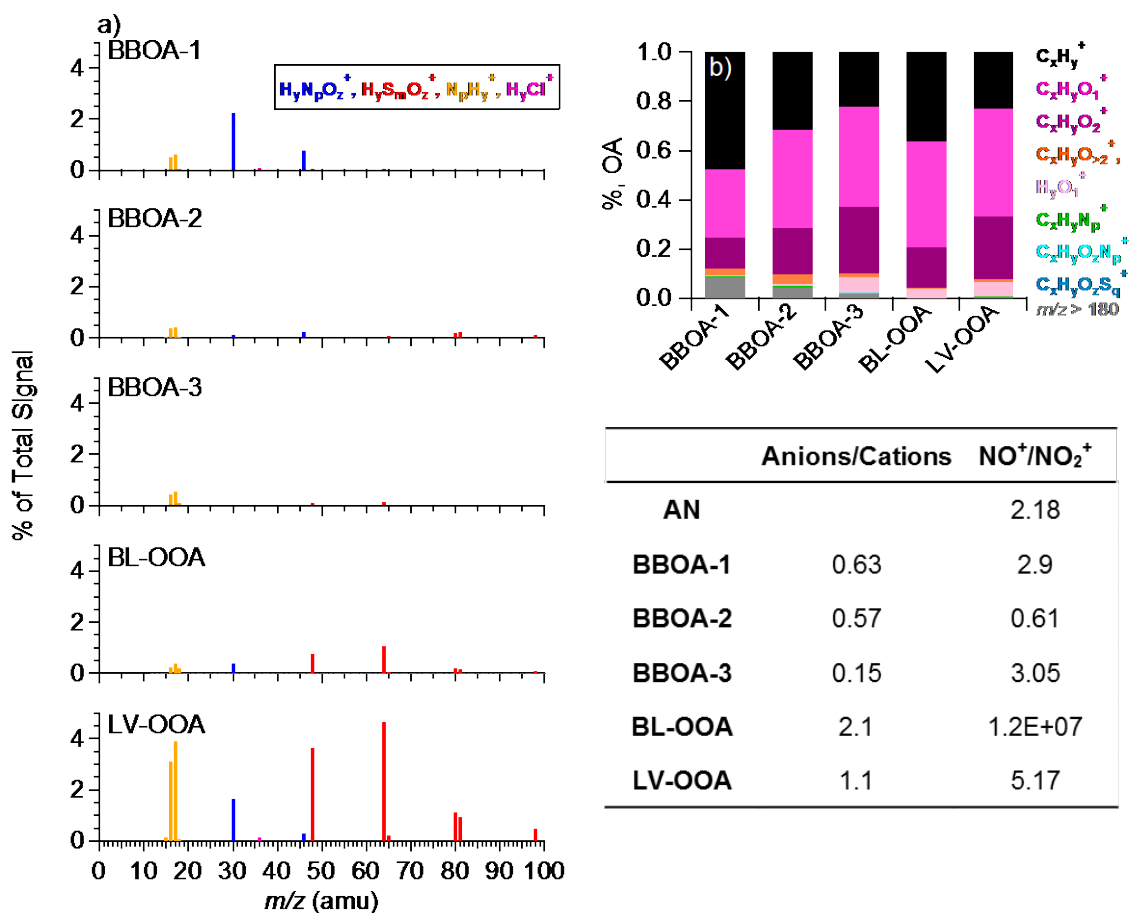
Fig. S11. (a) HRMS of inorganics and (b) OA composition colored by eight ion families and signal at $m/z > 180$ for each PMF factor. Table summarized the ratios of the molar equivalent of the sum of HR-AMS measured anionic species, i.e., sulfate, nitrate and chloride, to that of the cation species, ammonium (Anions/Cations) and NO^+ to NO_2^+ for pure ammonium nitrate (AN) and each PMF factor.
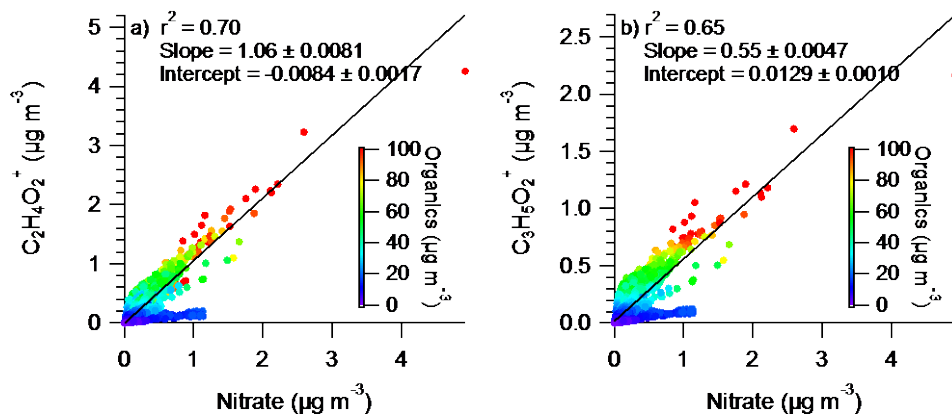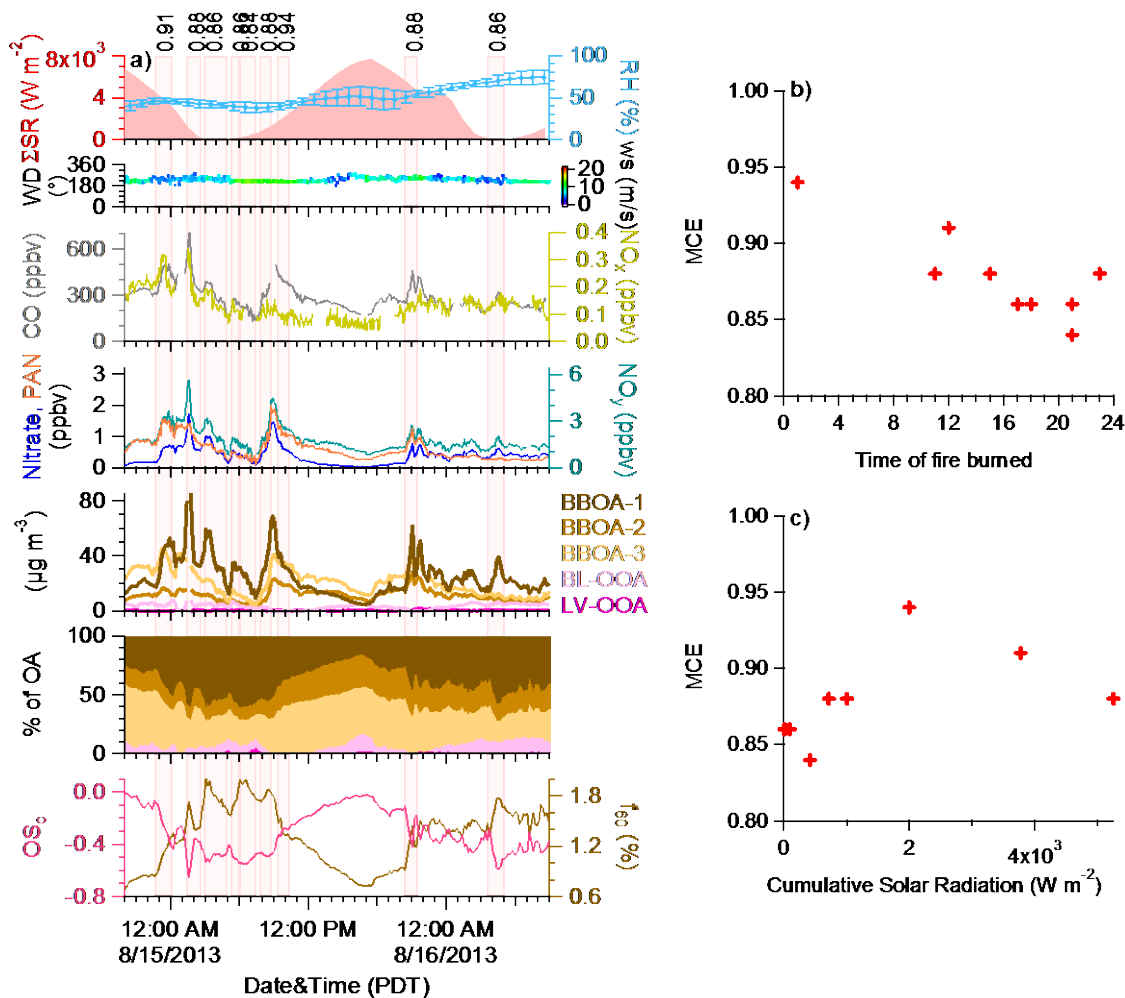
Fig. S12. Scatter plots of (a) $C_2H_4O_2^+$ and (b) $C_3H_5O_2^+$ versus nitrate, colored by organic mass concentrations. Data fitting was performed using the orthogonal distance regression (ODR).

Fig. S13. (a) The overview plot for the Salmon River Complex Fire Case Study (the right panel of Fig. 6) with 9 events calculated for modified combustion efficiency (MCE) highlighted. The numbers on the top are MCE values. (b) MCE values versus time of fire burned, and (c) MCE values versus Cumulative Solar Radiation for these 9 events.

98 **Reference**

99 Sun, Y. L., Zhang, Q., Schwab, J. J., Yang, T., Ng, N. L., and Demerjian, K. L.: Factor analysis of combined organic
100 and inorganic aerosol mass spectra from high resolution aerosol mass spectrometer measurements, Atmospheric
101 Chemistry and Physics, 12, 8537-8551, 2012.

102 Zhang, Q., Jimenez, J. L., Canagaratna, M. R., Ulbrich, I. M., Ng, N. L., Worsnop, D. R., and Sun, Y. L.:
103 Understanding atmospheric organic aerosols via factor analysis of aerosol mass spectrometry: a review, Anal.
104 Bioanal. Chem., 401, 3045-3067, 2011.

105